Discreteness-of-Charge Adsorption Micropotentials. I. Infinite Imaging

C. A. BARLOW, JR., AND J. ROSS MACDONALD
Texas Instruments Incorporated, Dallas, Texas 75222
(Received 2 October 1963)

The Ershler infinite imaging model for adsorption of ions from electrolytes is discussed in detail. An incorrect derivation of the basic equations for the micropotential is critically examined, and a correct derivation provided. The potential arising from discrete adions and their images is determined exactly based upon a method which heretofore has only been applied to crystal field problems. Finally, the accurate results obtained using a digital computer are compared with the approximate results of other treatments.

INTRODUCTION

THE present paper represents the first of a series treating the potential arising from adsorbed ions in various circumstances. In this first paper we are concerned with the situation where the ions are effectively "imaged" by two equipotential planes: This may come about when the adsorber is a good electrical conductor and the ions are adsorbed from a bulk "diffuse layer" of ions present in sufficient concentration to produce an approximately equipotential plane just beyond the adsorbed layer. This is a well-known state of affairs in electrolyte double-layer theory. When two equipotential planes are not maintained in such proximity, it is appropriate to consider another model: The single-image model is one such which is applicable to adsorption by a metal of ions from a gas phase. This model, which may be somewhat applicable to the electrolyte situation as well, will form the subject of the second paper of the series. There are cases where partial imaging (e.g., dielectric imaging) is appropriate; and this will be treated in the third paper of this series.

In any microscopic theory of adsorption of ions, a quantity which plays a fundamental part in determining the characteristics of the adsorption process is the electrochemical free energy of adsorption. This quantity, which itself depends upon the density and arrangement of the adsorbed phase, may be defined as the work required to move an ion of valency z from the bulk to a vacant adsorption position. Generally, this quantity depends upon the type of ion considered, the (metal) electrode, the charge on the metal, and to some extent the temperature of the system, as well as the structure of the adsorbed phase.

In the present work, we are concerned only with that part of the free energy which obtains when the detailed atomic structure of the ions and metal is ignored; that is, we confine attention to the ordinary electrostatic interactions, ignoring all ("chemical") interaction such as those arising from the possibility of internal structural changes of the ions themselves. Thus, that part of the free energy of adsorption we consider arises wholly from the Coulomb interaction between an adsorbed ion and all other adions and induced charges in the system. Another quantity related to but not identical with the free energy is often more useful in statistical adsorption theory: If one calculates the total Coulomb potential at the site of an adsorbed ion, discarding that ion's infinite direct contribution, the resulting potential is known as the micropotential, here denoted as ψ_1. Some previous discussion has recently been given of the micropotential and its use by various authors to calculate ionic adsorption by an ideal polarized electrode from the electrolyte double layer.[1] In the present work, we are solely concerned with potentials in the inner region of the double layer and not with the various forms of electrical adsorption isotherms in which the micropotential appears.

In early work,[2] the micropotential was calculated by ignoring discreteness-of-charge effects and thus by smearing the ions in the plane of adsorption, the inner Helmholtz plane (IHP). It therefore becomes in this approximation the mean potential at the IHP relative to the bulk of the electrolyte; and this approximate value of the micropotential is now generally known as the macropotential.[3]

In 1933, Frumkin[4] suggested that because of the actual discreteness of charge, the macropotential might be a poor approximation to the micropotential; and later Esin and Markov[5] seemed to verify this supposition indirectly by observing that the shift of the electrocapillary maximum (ecm) potential with increased adsorption of ions was larger than the shift predicted by the theory based on the macropotential. Since then, there have been many attempts to calculate ψ_1 approximately when charge discreteness in the IHP is not completely neglected. Esin and Shikov,[6] Grahame,[7] and Levine, Bell, and Calvert[8] have considered a model in which the adions are hexagonally arrayed, and in which a single equipotential plane (either the electrode or the outer Helmholtz plane (OHP), the plane of

[1] J. R. Macdonald and C. A. Barlow, Jr., Proc. 1st Australian Conf. Electrochemistry, Sydney, Australia, February 1963 (to be published).
[2] D. C. Grahame, Chem. Revs. **41**, 441 (1947) and references cited therein.
[3] B. V. Ershler, Zh. Fiz. Khim. **20**, 679 (1946).
[4] A. N. Frumkin, Phys. Z. Sowjetunion **4**, 256 (1933).
[5] O. Esin and B. Markov. Zh. Fiz. Khim. **13**, 318 (1939); Acta Phys. Chim. U.R.S.S. **10**, 353 (1939).
[6] O. Esin and V. Shikov, Zh. Fiz. Khim. **17**, 236 (1943).
[7] D. C. Grahame, Z. Elecktrochem. **62**, 264 (1958).
[8] S. Levine, G. M. Bell, and D. Calvert, Can. J. Chem. **40**, 518 (1962).

closest approach to the electrode of the charge centroids of ions in solution), serves as an imaging plane for the charges in the IHP. In all these treatments, the material (apart from the adions) present between the OHP and the electrode was replaced by a homogeneous medium of uniform dielectric constant ϵ. The analyses of these authors differed somewhat, but they agreed in yielding results which seemed to over explain the Esin–Markov effect. It was this dificiency which prompted the introduction by Ershler[3] of a somewhat different model whose consequences will principally comprise the subject of this paper.

In 1946, Ershler,[3] and later Grahame,[7] Levich, Kir'yanov, and Krylov,[9] and Levine, Bell and Calvert[8] analyzed a model in which both the adsorbing electrode and OHP are considered to be equipotential surfaces and hence perfect imaging planes. When these two planes both serve to image the hexagonally arrayed charges on the IHP, an infinite set of images results. The inclusion of this infinite imaging improved the agreement between theory and the Esin–Markov effect, which has lent some support to the model in spite of various approximations made in some of the calculations. On the other hand, it still seems quite possible that infinite imaging is basically inappropriate and that the necessary improvement of earlier models lies in other directions; thus, by way of example, the possibility remains open that the shift in the ecm arises partially from the orientation of dipoles in the polar solvent which occupies the inner layer, the region between the OHP and the electrode. There is already evidence[1,10] to support the existence of a significant solvent polarization in the inner layer at the ecm, although the exact causes for this dipole orientation are not yet completely understood. It is possible and even likely that the adions and/or diffuse layer of ions in solution play an important role in creating this inner layer polarization, in which case one might expect a consequent shift of the ecm with varying adion and/or diffuse layer concentration which differs from that predicted in the early single imaging treatments. A further possibility is that the dielectric constant in the inner layer varies significantly with position on either side of the IHP and that this too must be considered in any more accurate model of the inner layer. There is good reason to believe that this is true.[1,10] Further, even if one neglects imaging by the diffuse layer of ions, the approximate discontinuity of the dielectric constant of the solvent at the OHP or possibly between the IHP and OHP[1,11] will serve to image charges to some extent. Finally, the effects of thermal motion in the inner layer[12] and in the diffuse layer[9] could play a role in determining the relevance of an imaging model as well as other features of the system. We neglect thermal motion effects herein.

In this paper we shall consider in detail the simple infinite imaging model of Ershler,[3] Grahame,[7] Levich *et al.*,[9] and Levine *et al.*[8] giving an exact and computationally useful treatment of this model and at the same time presenting a method of calculating micropotentials which will be employed in subsequent papers treating different models. Before entering into the main stream of the paper, it is desirable first to present a correct derivation of the exact formulas applying to the simple infinite image (Ershler) model and to point out an error in the literature.

ERSHLER MODEL: INTRODUCTORY ANALYSIS AND COMPARISON WITH EARLIER TREATMENTS

We now consider the following model of the inner layer: Assume the adions to be hexagonally arrayed on the IHP with a nearest-neighbor distance r_1. Let β be the distance between the IHP and the adsorbing electrode, and define γ as the distance between the IHP and the OHP. Assume a mean charge per unit area q on the planar metal electrode which is exactly balanced by the adion charge per unit area q_1 at the IHP and the diffuse layer charge per unit area $-(q_1+q)$, considered as lying entirely on the OHP. Take the effective dielectric constant of the entire inner layer[13] as the constant ϵ, and assume that the OHP as well as the electrode is an equipotential surface. Finally, assume that the electrode and the charge-occupied areas of the IHP and OHP are of finite extent but are sufficiently large in dimension compared to β, γ, and r_1 that edge effects may be neglected over virtually all the occupied surface.

The question which now concerns us is: What is the electrical potential in the inner layer along the line which is perpendicular to the OHP and passes through the site where a single adion has been removed from the hexagonal array,[15] assuming that all other adions and their images remain undisturbed? One may pro-

[9] V. G. Levich, V. A. Kir'yanov, and V. S. Krylov, Proc. Acad. Sci. U.S.S.R. (Dokl. Akad. Nauk S.S.S.R.) Phys. Chem. Sec. **135,** 1193 (1960); V. S. Krylov, *ibid.* **144,** 356 (1962).

[10] J. R. Macdonald and C. A. Barlow, Jr., J. Chem. Phys. **36,** 3062 (1962).

[11] N. F. Mott, R. Parsons, and R. J. Watts-Tobin, Phil. Mag. **7,** 483 (1962).

[12] I. Langmuir, J. Am. Chem. Soc. **54,** 2798 (1932).

[13] The introduction of a dielectric constant is actually inappropriate to an essentially microscopic, discrete system such as that considered here and represents an approximation which will not be removed in the present work. Some discussion of how one more properly considers polarization effects in microscopic layers of one or more components is to be found elsewhere.[1,14] For the present work, we merely note that the "effective dielectric constant" introduced herein and involving polarization of the ions and surrounding molecules is not to be identified with any bulk value but is determined by the properties and arrangement in the inner layer of the discrete constituents. It follows that ϵ, insofar as it may be defined and taken position independent in the inner layer, will in general vary somewhat with q_1; this effect is likewise neglected here.

[14] J. R. Macdonald and C. A. Barlow, Jr., J. Chem. Phys. **39,** 412 (1963).

[15] Here, as in the following development, it is assumed that the event which takes place is sufficiently remote from the edge of the array that boundary effects may be ignored.

ceed in several ways to answer this question; here we adopt the method of images. We are assured that the electrode and the OHP are both equipotential surfaces by assuming that the potential in the inner layer, taken zero at the OHP,[16] is equal to the potential ψ_a which arises from the adions and infinite set of images (resulting from imaging in both electrode and OHP), plus the linearly varying potential ψ_e associated with a uniform field of as yet unknown magnitude. As we shall see, the field magnitude depends on both q and q_1. By the above assumption we also guarantee the satisfaction of the Poisson equation within the inner layer. Because of total charge neutrality, in the present model we may set the field outside the inner layer equal to zero. From the uniqueness theorem of electrostatics, the complete solution of the problem is found by determining the unknown linearly varying potential ψ_e to be added to ψ_a so that the resulting mean surface charge densities on both the metal and OHP are properly given as q and $-(q_1+q)$, respectively.

In order to determine the uniform field to be added, we must first answer the following important question: What are the mean surface charge densities q_{1m} and q_{1d} on the electrode and OHP associated with the potential ψ_a alone? These charges are readily determined by the following reasoning. First, we know by the vanishing of the field outside the inner layer and the applicability of Gauss's law that

$$q_{1m}+q_{1d}=-q_1. \tag{1}$$

That is, the total induced charge on the metal and OHP is just the negative of the inducing charge at the IHP; a well-known result. Next, by electrostatic theory we have a simple relation between the local surface charge density at any point on the surface and the normal component of electric field at that point on the surface. By averaging over the surface we obtain a relation between the average surface charge density associated with a field and the surface-averaged normal component of that field. In particular we find

$$4\pi q_{1m}/\epsilon=\langle E_m\rangle, \tag{2}$$

$$4\pi q_{1d}/\epsilon=\langle E_d\rangle, \tag{3}$$

where $\langle E_m\rangle$ and $\langle E_d\rangle$ are the surface-averaged normal components of the electric field at the metal and OHP, respectively. In both cases the surface normal is chosen directed towards the IHP.

The averages in Eqs. (2) and (3) are most easily determined by observing that the surface-averaged field is equal to just that field which would result from smearing the source charges in their planes.[17] We therefore may write

$$-4\pi q_1/\epsilon=\langle E_m\rangle+\langle E_d\rangle; \tag{4}$$

and because $\psi_a=0$ on both the metal and OHP (by construction of the images),

$$\langle E_m\rangle\beta=\langle E_d\rangle\gamma. \tag{5}$$

We may solve (4) and (5) to yield

$$\langle E_m\rangle=-(4\pi q_1/\epsilon)[\gamma/(\beta+\gamma)], \tag{6}$$

and

$$\langle E_d\rangle=-(4\pi q_1/\epsilon)[\beta/(\beta+\gamma)]. \tag{7}$$

By substitution into (2) and (3), we find

$$q_{1m}=-[\gamma/(\beta+\gamma)]q_1, \tag{8}$$

and

$$q_{1d}=-[\beta/(\beta+\gamma)]q_1. \tag{9}$$

Now we are ready to determine ψ_e. Letting the electrode and the OHP define the planes $x=+(\beta+\gamma)$ and $x=0$, respectively, one may write

$$\psi_e(x)=E_e x, \tag{10}$$

where E_e is the uniform field to be determined. By Gauss's law, associated with this field are the constant mean surface charge densities σ_{qm} and σ_{qd} on the metal and OHP, respectively, given by the expressions

$$\sigma_{qm}=\epsilon E_e/4\pi, \tag{11}$$

$$\sigma_{qd}=-\epsilon E_e/4\pi. \tag{12}$$

We may satisfy the remaining conditions

$$q_{1m}+\sigma_{qm}=q,$$

$$q_{1d}+\sigma_{qd}=-(q+q_1),$$

simply by setting

$$E_e=(4\pi/\epsilon)[q+q_1\{\gamma/(\beta+\gamma)\}]. \tag{13}$$

The complete potential at the position x is now obtained by adding to $\psi_e(x)$ the contribution $\psi_a(x)$ from the discrete lattice of ions and their images; recall that this lattice contains a vacancy at one ion position ($x=\gamma$) and at all associated image positions which lie on the line perpendicular to the adsorbing surface passing through the ion vacancy site. Later we present a technique for calculating ψ_a accurately, but for the present we note that most other authors have been concerned with obtaining approximate, but readily calculable expressions for ψ_a: The basic problem is that a direct summation of the contributions from each lattice point takes practically forever to converge.

The complete micropotential should of course contain the contribution from the interaction of an adion with its line of self-images; we omit this in the remainder of the present work because it is divergent

[16] The p.d. between the OHP and the bulk of the solution, V_2, is thus omitted from the definition of the micropotential but may be included whenever appropriate.

[17] N. F. Mott and R. J. Watts-Tobin, Electrochim. Acta **4**, 79 (1961).

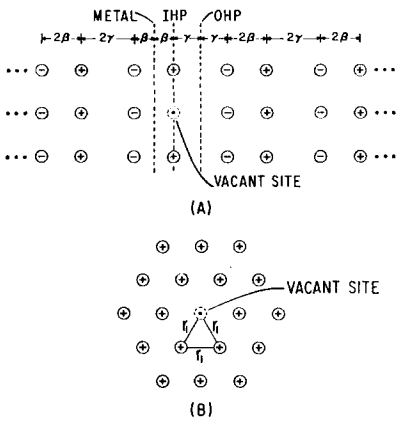

FIG. 1. Lattice of ions and images: (a) ⊥ IHP; (b) IHP.

for the ideal Ershler model; since it is independent of q_1 and q, it can be considered as part of the chemical free energy of adsorption in any case. With this in mind, and because from symmetry $\psi_a(0)=\psi_e(0)=0$, we may write the micropotential ψ_1 as follows:

$$\begin{aligned}\psi_1&=\psi_a(\gamma)+\psi_e(\gamma)-\{\psi_a(0)+\psi_e(0)\}\\&=\psi_a(\gamma)+\psi_e(\gamma)\\&=\psi_a(\gamma)+(4\pi\gamma/\epsilon)[q+q_1\{\gamma/(\beta+\gamma)\}].\end{aligned}\quad(14)$$

Before considering ψ_a in more detail, let us make several observations on the results obtained so far and make comparisons with Grahame's[7] treatment. First, one should note that the total p.d. across the inner layer, V_1, does not involve ψ_a, because $\psi_a=0$ both on the metal and on the OHP for infinite imaging. We therefore have that

$$\begin{aligned}V_1=\psi_e(\beta+\gamma)&=(\beta+\gamma)E_e\\&=(4\pi/\epsilon)[q+\{\gamma/(\beta+\gamma)\}q_1](\beta+\gamma).\end{aligned}\quad(15)$$

At the ecm, $q=0$, and $V_1=(4\pi q_1\gamma)/\epsilon$. It is sometimes convenient to subtract this quantity from the true p.d. in order to obtain a shifted p.d. which is zero at the ecm. Such a shift will have no effect on quantities which depend only upon p.d. differences; but for quantities which depend upon the absolute value of the p.d., this shift must be eliminated. Secondly, to the extent that one may neglect ψ_a, the field in the inner layer is uniform, and hence the micropotential is just given by

$$\psi_1\simeq[\gamma/(\beta+\gamma)]V_1.\quad(16)$$

Grahame[7] has obtained the equivalent of (15) and (16); however, his derivation is faulty. His first error is to assume that at the ecm ($q=0$) the potential in the inner layer arises purely from the adions and their infinite set of images. We have already seen, however, that in order that the potential be so given the average charge density on the electrode must be $q=-q_1\gamma/(\beta+\gamma)$; thus at the ecm where $q=0$ there is an amount of charge density $q_1\gamma/(\beta+\gamma)$ which is not accounted for. His second error is in finding a finite contribution to the total inner layer p.d., V_1, from the discrete potential ψ_a; this contribution Grahame initially ($q=0$) denotes as ψ^u. We have seen that $\psi_a=0$ on both the metal and the OHP and hence that ψ^u should be zero. Grahame's method of calculation when properly applied does, in fact, produce this vanishing ψ^u provided one considers a lattice finite in extent over the IHP. By implicitly considering an infinite lattice and carrying out the summations in such an order that the resulting ψ_a does not actually converge, he obtains a manifestly incorrect expression for $\psi^u=\psi_a(\beta+\gamma)-\psi_a(0)$. That his expression predicting finite values for ψ^u is incorrect should have been apparent through several means: First, ψ^u should have been invariant under interchange of β and γ; secondly, his equation would predict a finite p.d. between two grounded conductors, whereas the whole method of construction of images in the first place is such that the resulting ψ_a is actually assured of vanishing on the two imaging planes.

His third error is actually a repetition of the first: When he finds the effect of $q\neq0$, he neglects the fact that parts of the total average charge densities on the electrode and the OHP are involved in setting up the images which lead to ψ_a. The charge on the electrode, therefore, has already been partially taken into account and is not completely identical with the charge participating in production of the uniform field. A similar statement holds for the charge on the OHP. The result of this error is to produce an incorrect value for Grahame's ψ^{02} [equivalent to $\psi_e(\beta+\gamma)-\psi_e(0)$ in the present work]. This error is just compensated by the earlier ones involving the infinite-image potential, which Grahame now defines as ψ^v for the case $q\neq0$, and the correct value of V_1 (now expressed by $\psi^u\equiv\psi^v+\psi^{02}$) is obtained for any q.

Finally, to obtain the micropotential Grahame makes the approximation that the field in the inner layer is uniform. In this manner Eq. (16) is obtained. As we have seen, however, (16) gives the *exact* expression for the micropotential if one completely neglects $\psi_a(\gamma)$, the infinite image potential. Because Grahame obtains a contribution to V_1 from this potential, it would seem at first sight that by the uniform field approximation his treatment determines approximately the effect of ψ_a; actually, because ψ_a contributes exactly nothing to V_1 the uniform field approximation is tantamount

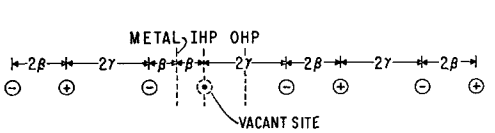

FIG. 2. Some of the self-image charges whose contributions will be subtracted out.

to the neglect of ψ_a entirely, an approximation which may frequently be poor, as shown later.

DISCRETE-CHARGE POTENTIAL: ψ_a

We turn now to the calculation of ψ_a. Recall that the potential desired is that produced by the lattice of charges resulting from the infinite imaging of a hexagonal array of adions with one vacancy. This potential (referred to zero potential at the OHP) may be formally written for a hexagonal lattice as a simple sum of Coulomb potentials in a not unfamiliar way:

$$\psi_a(\gamma)=\frac{6ze}{\epsilon}\sum_{l=-\infty}^{\infty}\sum_{m=1}^{\infty}\sum_{n=0}^{m-1}[r_1^2(m^2+n^2-mn)+4l^2(\beta+\gamma)^2]^{-\frac{1}{2}}$$
$$-\{r_1^2(m^2+n^2-mn)+4[(\beta+\gamma)l-\beta]^2\}^{-\frac{1}{2}}, \quad (17)$$

where $z \equiv$ valence of adion, and $e \equiv$ charge of proton. Because of the exceedingly slow convergence of this sum, however, we find it more convenient first to determine (by somewhat devious means) the potential ϕ_a arising from the lattice of charges with one vacant adion site but with all image sites occupied. We may then readily determine ψ_a by subtracting out the contribution from the added self-image charges. Figure 1 illustrates the lattice of charges for which we will find the potential $\phi_a(\mathbf{R})$ along the normal line through the origin. Figure 2 shows some of the charges whose contributions to ϕ_a must be subtracted in order to obtain ψ_a. The vectors we use in describing the lattice are presented in Fig. 3.

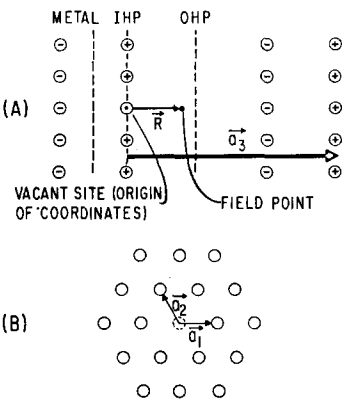

FIG. 3. Lattice basis vectors: (a) ⊥ IHP; (b) IHP.

Referring to the figures, the potential $\phi_a(\mathbf{R})$ may be written

$$\phi_a(\mathbf{R})=-\frac{ze}{\epsilon\,|\,[\beta/(\beta+\gamma)]\mathbf{a}_3+\mathbf{R}\,|}+\frac{ze}{\epsilon}\sum_{\mathbf{k}}{}'\{|\,\mathbf{r}_{\mathbf{k}}-\mathbf{R}\,|^{-1}-|\,\mathbf{r}_{\mathbf{k}}-[\beta/(\beta+\gamma)]\mathbf{a}_3-\mathbf{R}\,|^{-1}\}. \quad (18)$$

In Eq. (18), the primes on the summations refer to the exclusion of the lattice point at the origin; all other lattice points, $\mathbf{r}_{\mathbf{k}}\equiv k_1\mathbf{a}_1+k_2\mathbf{a}_2+k_3\mathbf{a}_3$ (k_1, k_2, k_3 all integers), are summed over.

There have been numerious methods developed for calculating lattice sums of the type occurring in Eq. (18). The main difficulty is that a straightforward attempt to compute such sums by direct addition fails to converge adequately in less than an astronomical number of terms. As a consequence, various approximations have evolved: Generally these approximations involve summing certain terms exactly and replacing the remainder by an integral. Representative of this approach is the excellent work of Levine, Bell, and Calvert[8] based on a method suggested by Grahame.[7] Yet another method, the one applied here, was originated by Ewald[18] and has been used in the past to calculate Madelung constants for ionic crystals:[19,20] This is a natural method to use here when one notes the similarity between the present problem and that of calculating fields in such crystals. Note, however, that the different assignment of charge signs here from that to be found in a typical crystal field problem makes the convergence properties of the simple series such as that in Eq. (18) even worse, thereby further necessitating the use of special techniques to obtain significant numerical results.

In Appendix I an analysis is given leading to a rapidly convergent form for $\phi_a(\mathbf{R})$ as well as for the self-image contribution. Comparison with the Ewald method[18] as generalized by de Wette[20] would reveal substantial additional complications encountered here as a result of the type of "lattice" of charge arising from the present infinite imaging situation. Appendix I is intended to be self-contained, however, in the sense that the reader need not refer for background information to the work of Ewald and de Wette.

The potential $\psi_a(\gamma)$ is found by subtracting the self-image contribution $S_0(0)$ from $\phi_a(0)$, these quantities being given in Appendix I, to yield

$$\psi_a(\gamma)=\phi_a(0)-\frac{ze}{2\epsilon(\beta+\gamma)}\left\{2\gamma_1+\psi\left(\frac{\beta}{\beta+\gamma}\right)+\psi\left(\frac{\gamma}{\beta+\gamma}\right)\right\}. \quad (19)$$

(It may be shown that the value of ψ_a is invariant under the interchange $\beta\leftrightarrow\gamma$ as required.) The micropotential ψ_1 follows immediately from (14). Equation (19) combined with Eqs. (I.20) and (14) represents a complete solution for the micropotential in the sense

[18] P. P. Ewald, Ann. Phys. **54**, 519, 557 (1917); **64**, 253 (1921); Nach. Ges. Wiss. Göttingen **55**, (1938).
[19] J. Sherman, Chem. Rev. **10–11**, 93 (1932).
[20] F. W. de Wette, Ph.D. thesis, University of Utrecht (1959); Physica **23**, 309 (1957); **24**, 422, 1105 (1958).

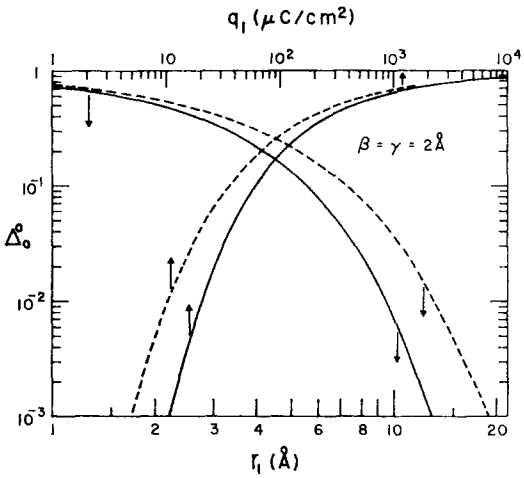

FIG. 4. Normalized discreteness contribution Δ_0^0 vs adsorption-layer charge density.

that the computation may now be carried out numerically with rapid convergence to an answer. For a hexagonal lattice, we also need the following relations between r_1 and q_1:

$$q_1 = (2/\sqrt{3})ze r_1^{-2} = 1.8499\times10^{-13} z r_1^{-2}; \quad (20)$$

$$r_1 = (4/3)^{\frac{1}{2}}(ze/q_1)^{\frac{1}{2}} = 4.3010\times10^{-7}(z/q_1)^{\frac{1}{2}}, \quad (21)$$

where in the numerical equations r_1 is in cm and q_1 in μC/cm.^{2} The "cut-off" radius r_0 used by Levine *et al.*[8] is 0.52605 r_1.

Finally, it is worth pointing out that a very valuable check on the analysis and numerical calculation of $\phi_a(0)$ is afforded by variation of the length parameter s employed in Appendix I. The results must be independent of s; if calculations with two s values yield the same numerical value of $\phi_a(0)$ to four or five significant figures, the probability of the answer being correct is exceedingly high. In the present work, s was usually taken of the order of r_1, but several values were always used for each calculated point and agreement of results was very good.

CALCULATED RESULTS AND COMPARISONS

The Grahame approximation, Eq. (16), states that the micropotential ψ_1 and the average potential across the entire inner layer, V_1, are directly proportional for all q_1 values. Experimentally,[21,22] the proportionality factor is found to vary appreciably with q_1; this behavior has recently been discussed by Parry and Parsons[23] and by the present authors.[1] Although the infinite imaging model analyzed herein is rather idealized, its predictions of ψ_1/V_1 are still more relevant to the experimental results than those of any previous calculations.

To achieve maximum generality, it is desirable to use normalized variables. Let us therefore define

$$\psi_1/V_1 \equiv [\gamma/(\beta+\gamma)][1+\Delta], \quad (22)$$

where from (14) and (15)

$$\Delta \equiv \frac{\psi_a(\gamma)}{(4\pi\gamma/\epsilon)}\left[q + q_1\left\{\frac{\gamma}{(\beta+\gamma)}\right\}\right]. \quad (23)$$

Note that Δ may also be expressed as

$$\psi_a(\gamma)/[\psi_1 - \psi_a(\gamma)].$$

We are particularly interested in how Δ depends on q_1 or r_1 for various values of β/γ and q. Let us therefore define Δ_0 as the value of Δ when $q\equiv0$, Δ^0 as the value when $\beta=\gamma$, and Δ_0^0 as the value when $q=0$ and $\beta=\gamma$. We are primarily concerned with Δ_0 since only approximate results are available from experiment for $q_1(q)$.

One of the advantages of dealing with Δ or Δ_0 rather than ψ_1 directly is that Δ is independent of ϵ on the present model. Even when it is reasonable to take ϵ dependent on q and q_1, such dependence cancels out of Δ since $\psi_a(\gamma) \propto \epsilon^{-1}$. As well as being the value of Δ when $q=0$, Δ_0 is also the limit of Δ when q is held fixed at some nonzero value and $|z| \to \infty$. When $q=0$, $\Delta \equiv \Delta_0$ does not depend on z at all. In the limits $q_1 \to 0$ ($r_1 \to \infty$) and $q_1 \to \infty$ ($r_1 \to 0$), it may be shown that $\Delta_0 \to 0$ and β/γ, respectively.

A variety of accurate values of Δ have been calculated using a digital computer. The results for Δ_0^0 are shown in Fig. 4 for the typical values $\beta=\gamma=2$ Å. The accurate curves, shown solid, are plotted vs both r_1 and q_1 (for positive adions). The results of the approximate cut-off treatment of Levine *et al.*[8] are shown dashed. These authors developed a very slowly convergent single series for $\psi_a(\gamma)$ applying when $\beta=\gamma$ and transformed the series analytically to a more rapidly convergent series in the range $r_0 > (\beta+\gamma)$. It is worth noting that to obtain numerical results this lengthy analytical work was unnecessary. Instead, the ϵ algorithm[24] could have been applied to the first few terms of the original, slowly convergent series to yield an accurate value for the sum of the entire series. This approach has the further virtue that it is applicable for much smaller values of $r_0/(\beta+\gamma)$ than unity. For example, for $r_0/(\beta+\gamma)=0.1$, the first three terms of the original series yield, using the ϵ algorithm, a result for the sum correct to 1%, while the first five terms lead to a result accurate to 0.03%. Unfortunately, the present exact triple series cannot be summed by the ϵ algorithm or its variants.[25]

Figure 4 shows that the cut-off approach consistently overestimates Δ_0^0. It predicts a value about 2.4 times too large at $q_1=40$ μC/cm,^{2} about the maximum

[21] D. C. Grahame, J. Am. Chem. Soc. **80**, 4201 (1958).
[22] D. C. Grahame and R. Parsons, J. Am. Chem. Soc. **83**, 1291 (1961).
[23] J. M. Parry and R. Parsons, Trans. Faraday Soc. **59**, 241 (1963).
[24] P. Wynn, Chiffres **4**, 23 (1961); Math. Comp. **15**, 151 (1961); Mathematics Tables and Other Aids to Computation **10**, 91 (1956).
[25] D. Shanks, J. Math. and Phys. **34**, 1 (1955).

experimental value, and 12 times too large at $q_1=10$ μC/cm.^{2} From the magnitudes of the accurate values of Δ_0^0 in the present $\beta=\gamma=2$ Å case, it is clear that ψ_1 and V_1 are proportional over the entire experimental range of q_1 to within 5% accuracy. The concomitant variation of q with q_1 found experimentally makes Δ rather than Δ_0 the quantity of most interest for comparison with experiment in the electrolyte case. Some consideration of Δ is given later.

Let us now consider the Δ_0 results for various ratios: (β/γ). It has been found that the results can be represented most economically by plotting Δ_0 as a function of r_1/ξ, where ξ is the smaller of β and γ. Typical accurate results are presented in Fig. 5. The parameters shown on the curves are the values of β/γ. The curve for $\beta=\gamma$ is shown solid, those for $\beta<\gamma$ dotted, and those for $\beta>\gamma$ dashed. It will be noted that the curve

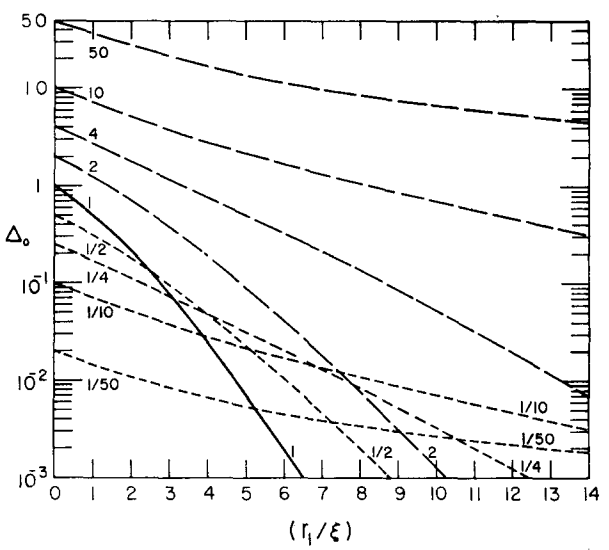

FIG. 5. Normalized discreteness contribution Δ_0 for various ratios r_1/β and r_1/γ.

for $\beta=\gamma$ represents the limiting case; all other curves have smaller slope magnitudes. Another result, which simplifies the construction of curves, is that curves for $\beta/\gamma=a>1$ are of exactly the same shape, on a semilog plot, as those for $\beta/\gamma=a^{-1}$, the only difference being a vertical displacement by a factor a^2 when passing from the $\beta/\gamma=a$ curves to those with $\gamma/\beta=a$.

It is interesting to note that the results of Fig. 5 show that the curves change from convex to the abscissae to concave between $\beta/\gamma=4$ and 10. Between these values lies a curve which is very nearly pure exponential in its dependence on r_1/ξ. Experimentally likely values of β/γ in the electrolyte situation lie between about 4 and 1/4. Note that the $\beta/\gamma=4$ curve involves values of Δ_0 which are much too large to neglect even for appreciable values of r_1/ξ. In such situations, the Grahame approximation is invalid. The cut-off solution of Levine *et al.*[8] is only applicable when $\beta=\gamma$ and so cannot be compared with the $\beta\neq\gamma$

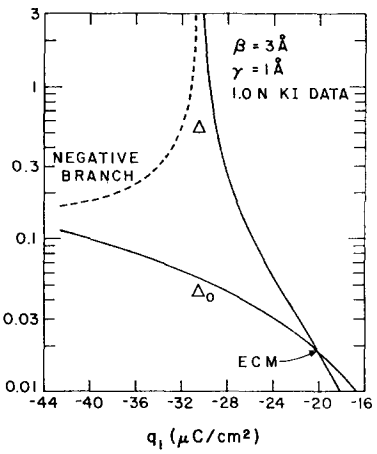

FIG. 6. Normalized discreteness contribution Δ vs Grahame's derived $q_1(q)$: $\beta=3$ Å, $\gamma=1$ Å.

curves of Fig. 5. Unfortunately, the apparently exact, but still slowly convergent, solution of Levich *et al.*[9] for ψ_1 has not been sufficiently reduced to numerical or graphical results for comparison with those of the present work.

Finally, Figs. 6 and 7 show how Δ varies with q_1 according to the present model when $q_1(q)$ data derived by Grahame[21] from his measurements of differential capacitance of 1.0 N KI are used. Also shown are the corresponding curves for Δ_0. Figure 6 shows the results when $\beta=3$ Å and $\gamma=1$ Å, values recently used by Parry and Parsons[23] for another electrolyte. The contributions to β and γ have been discussed elsewhere by the authors,[1,10] and it is suggested that a treatment of double-layer capacitance when ions are specifically adsorbed should involve a distinction between regions near a specifically adsorbed ion and regions appreciably away from such ions. Such distinction makes it impossible to assign a unique thickness to the inner part of the double layer since the OHP is no longer really a plane. If one considers only the value for γ near an adsorbed ion, one might expect it to in-

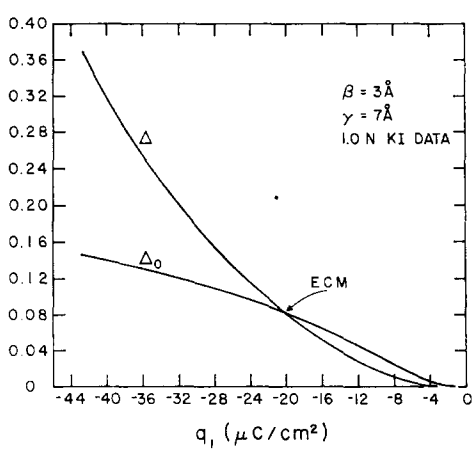

FIG. 7. Normalized discreteness contribution Δ vs Grahame's derived $q_1(q)$: $\beta=3$ Å, $\gamma=7$ Å.

clude as a maximum approximately a radius of the adion, the diameter of a hydrated water molecule between the adion and an ion in the diffuse layer at the OHP, and approximately the radius of this ion. Although this appreciable thickness may be somewhat reduced as far as capacitance and average potential calculations are concerned by supposing with Mott, Parsons, and Watts-Tobin[11] that the dielectric constant rises rapidly in the inner layer with distance from the electrode, it seems unlikely that γ could be as small as 1 Å. Figure 6 seems to indicate that the values $\beta=3$ Å and $\gamma=1$ Å are a very poor approximation to the truth for KI since they lead to an infinite value for Δ (implying a zero value of V_1) within the experimental q_1 range. Note that a logarithmic scale for Δ is used in this figure and that negative values of Δ are shown reversed in sign and dashed.

The more reasonable values $\beta=3$ A and $\gamma=7$ A are used for the curves of Fig. 7. Here the ordinate scale is linear and no pole in Δ appears in the experimental range. The value $\gamma=7$ Å is probably the maximum value which might be expected for KI on the basis of the contributions discussed in the preceding paragraph. If $\beta\sim3$ A and 1 Å$<\gamma<7$ A, then Δ will increase faster than that of Fig. 7. The trend of Δ vs q_1 of Fig. 7 is in qualitative agreement with the dependence of ψ_1/V_1 found by various authors using (16) or variants thereof together with rather inaccurate expressions for obtaining ψ_1 and V_1 from experimental data. No quantitative comparison is justified at present because of the inaccuracy of the expressions which have been used to obtain ψ_1/V_1 from the experimental data thus far.

ACKNOWLEDGMENTS

The authors gratefully acknowledge the assistance of Michiel de Wit, who recommended that crystal field methods might be useful in micropotential calculations, and of Charles Ratliff, who wrote the program for performing the necessary calculations on a digital computer.

APPENDIX I: LATTICE SUM

We may rewrite Eq. (18) as

$$\phi_a(\mathbf{R})=-\frac{ze}{\epsilon\,|\,[\beta/(\beta+\gamma)]\mathbf{a}_3+\mathbf{R}\,|}+\frac{ze}{\epsilon s}\sum_{\mathbf{k}}{}'\left\{\frac{1}{|\,\xi_{\mathbf{k}}-\zeta\,|}-\frac{1}{|\,\xi_{\mathbf{k}}-[\beta/(\beta+\gamma)]\mathbf{f}_3-\zeta\,|}\right\},\tag{I1}$$

where $s\equiv$ an arbitrary length,

$$\xi_{\mathbf{k}}\equiv s^{-1}\mathbf{r}_{\mathbf{k}}\equiv k_1\mathbf{f}_1+k_2\mathbf{f}_2+k_3\mathbf{f}_3,$$
$$\mathbf{f}_i\equiv s^{-1}\mathbf{a}_i\qquad(i=1,2,3),$$
$$\zeta\equiv s^{-1}\mathbf{R}.$$

We next produce the equality

$$\phi_a(\mathbf{R})=-\frac{ze}{\epsilon\,|\,[\beta/(\beta+\gamma)]\mathbf{a}_3+\mathbf{R}\,|}+\frac{ze}{\epsilon s}\sum_{\mathbf{k}}{}'\left\{\frac{\mathrm{Erfc}(\pi^{\frac{1}{2}}\,|\,\xi_{\mathbf{k}}-\zeta\,|)}{|\,\xi_{\mathbf{k}}-\zeta\,|}-\frac{\mathrm{Erfc}(\pi^{\frac{1}{2}}\,|\,\xi_{\mathbf{k}}-[\beta/(\beta+\gamma)]\mathbf{f}_3-\zeta\,|)}{|\,\xi_{\mathbf{k}}-[\beta/(\beta+\gamma)]\mathbf{f}_3-\zeta\,|}\right\}$$
$$+\frac{ze}{\epsilon s(\pi)^{\frac{1}{2}}}\sum_{\mathbf{k}}{}'\left\{\frac{\gamma(\frac{1}{2},\pi\,|\,\xi_{\mathbf{k}}-\zeta\,|^2)}{|\,\xi_{\mathbf{k}}-\zeta\,|}-\frac{\gamma(\frac{1}{2},\pi\,|\,\xi_{\mathbf{k}}-[\beta/(\beta+\gamma)]\mathbf{f}_3-\zeta\,|^2)}{|\,\xi_{\mathbf{k}}-[\beta/(\beta+\gamma)]\mathbf{f}_3-\zeta\,|}\right\},\tag{I2}$$

where

$$\mathrm{Erfc}(x)\equiv 1-\mathrm{Erf}(x)\equiv 1-\frac{2}{\pi^{\frac{1}{2}}}\int_0^x\exp(-t^2)\,dt,$$
$$\gamma(n,x)\equiv\Gamma(n)-\Gamma(n,x),$$
$$\gamma(\tfrac{1}{2},x^2)\equiv\pi^{\frac{1}{2}}\,\mathrm{Erf}(x),$$

and should not be confused with the distance, γ, and

$$\Gamma(n,x)\equiv\int_x^\infty e^{-t}t^{n-1}dt.$$

In Eq. (I2) the first summation may be made to converge rapidly by choosing a sufficiently small value for s. The problem remaining is to evaluate the second summation. It is this task which now forms a major digression.

We write

$$I_1(\mathbf{R})\equiv\frac{ze}{\epsilon s(\pi)^{\frac{1}{2}}}\sum_{\mathbf{k}}{}'\left(\frac{\gamma(\frac{1}{2},\pi\,|\,\xi_{\mathbf{k}}-\zeta\,|^2)}{|\,\xi_{\mathbf{k}}-\zeta\,|}-\frac{\gamma(\frac{1}{2},\pi\,|\,\xi_{\mathbf{k}}-[\beta\mathbf{f}_3/(\beta+\gamma)]-\zeta\,|^2)}{|\,\xi_{\mathbf{k}}-[\beta/(\beta+\gamma)]\mathbf{f}_3-\zeta\,|}\right)$$
$$=\frac{ze}{\epsilon s(\pi)^{\frac{1}{2}}}\int d^3\xi\left\{\frac{\gamma(\frac{1}{2},\pi\,|\,\xi-\zeta\,|^2)}{|\,\xi-\zeta\,|}-\frac{\gamma(\frac{1}{2},\pi\,|\,\xi-[\beta/(\beta+\gamma)]\mathbf{f}_3-\zeta\,|^2)}{|\,\xi-[\beta/(\beta+\gamma)]\mathbf{f}_3-\zeta\,|}\right\}\sum_{\mathbf{k}}{}'\delta(\xi-\xi_{\mathbf{k}}),\tag{I3}$$

where $\delta(\mathbf{x}) \equiv$ Dirac δ function. If one now defines the reciprocal lattice basis vectors, $\mathbf{b}_1$, $\mathbf{b}_2$, $\mathbf{b}_3$, as follows:

$$\mathbf{b}_1 \equiv \frac{\mathbf{a}_2 \times \mathbf{a}_3}{\mathbf{a}_1 \cdot \mathbf{a}_2 \times \mathbf{a}_3} = \frac{\mathbf{a}_2 \times \mathbf{a}_3}{(\beta+\gamma) r_1^2 \sqrt{3}}$$

$$\mathbf{b}_2 \equiv \frac{\mathbf{a}_3 \times \mathbf{a}_1}{\mathbf{a}_1 \cdot \mathbf{a}_2 \times \mathbf{a}_3} = \frac{\mathbf{a}_3 \times \mathbf{a}_1}{(\beta+\gamma) r_1^2 \sqrt{3}}$$

$$\mathbf{b}_3 \equiv \frac{\mathbf{a}_1 \times \mathbf{a}_2}{\mathbf{a}_1 \cdot \mathbf{a}_2 \times \mathbf{a}_3} = \frac{\mathbf{a}_1 \times \mathbf{a}_2}{(\beta+\gamma) r_1^2 \sqrt{3}}$$

and the associated vectors $\mathbf{g}_i \equiv s\mathbf{b}_i (i=1, 2, 3)$, one finds the following relations:

$$\mathbf{f}_i \cdot \mathbf{g}_j = \delta_{ij}; \tag{I4}$$

$$| \mathbf{f}_1 | = | \mathbf{f}_2 | = r_1/s, \qquad | \mathbf{f}_3 | = 2(\beta+\gamma)/s; \tag{I5}$$

$$| \mathbf{g}_1 | = | \mathbf{g}_2 | = \frac{2s}{\sqrt{3} r_1}, \qquad | \mathbf{g}_3 | = s/(2\beta+2\gamma); \tag{I6}$$

$$\mathbf{g}_1 \cdot \mathbf{g}_3 = \mathbf{g}_2 \cdot \mathbf{g}_3 = \mathbf{f}_1 \cdot \mathbf{f}_3 = \mathbf{f}_2 \cdot \mathbf{f}_3 = 0 \qquad \mathbf{f}_1 \cdot \mathbf{f}_2 = -\tfrac{1}{2}(r_1/s)^2, \qquad \mathbf{g}_1 \cdot \mathbf{g}_2 = \tfrac{2}{3}(s/r_1)^2. \tag{I7}$$

Finally, we require the normalized reciprocal lattice vectors $\mathbf{h}_\lambda \equiv \lambda_1 \mathbf{g}_1 + \lambda_2 \mathbf{g}_2 + \lambda_3 \mathbf{g}_3$, where λ_1, λ_2, λ_3 are integers.

The trick we use in evaluating I_1 is to note Parseval's theorem:

$$\int d^3x \Phi_1^*(\mathbf{x}) \Phi_2(\mathbf{x}) = \int d^3h G_1^*(\mathbf{h}) G_2(\mathbf{h}),$$

where

$$G(\mathbf{h}) \equiv \mathfrak{F}_3\{\Phi\} \equiv \int d^3x \Phi(\mathbf{x}) \exp\{-2\pi i \mathbf{h} \cdot \mathbf{x}\}.$$

We show in Appendix II that the Fourier transform of

$$\sum_{\mathbf{k}}{}' \delta(\xi - \xi_{\mathbf{k}})$$

is given by

$$\frac{1}{v_f} \sum_{\lambda} \delta(\mathbf{h} - \mathbf{h}_\lambda) - 1,$$

where

$$v_f \equiv \mathbf{f}_1 \cdot \mathbf{f}_2 \times \mathbf{f}_3 = s^{-3} r_1^2 \sqrt{3} (\beta+\gamma).$$

The Fourier transform of $\pi^{-\frac{1}{2}} | \xi |^{-1} \gamma(\frac{1}{2}, \pi | \xi |^2)$ is known to be $\pi^{-1} | \mathbf{h} |^{-2} \exp\{-\pi | \mathbf{h} |^2\}$; thus the transform of

$$\frac{\gamma(\frac{1}{2}, \pi | \xi - \mathbf{n} |^2)}{\pi^{\frac{1}{2}} | \xi - \mathbf{n} |}$$

is

$$\exp\{2\pi i \mathbf{h} \cdot \mathbf{n}\} \exp\{-\pi | \mathbf{h} |^2\}/\pi | \mathbf{h} |^2.$$

Making use of Parseval's theorem we easily obtain

$$I_1(\mathbf{R}) = \frac{ze}{\epsilon s} \int d^3h \left\{ \left[\exp\{-2\pi i \mathbf{h} \cdot \zeta\} - \exp\left\{ -2\pi i \mathbf{h} \cdot \left(\frac{\beta}{\beta+\gamma} \mathbf{f}_3 + \zeta \right) \right\} \right] \frac{\exp\{-\pi | \mathbf{h} |^2\}}{\pi | \mathbf{h} |^2} \left[\frac{s^3}{(\beta+\gamma) r_1^2 \sqrt{3}} \sum_{\lambda} \delta(\mathbf{h} - \mathbf{h}_\lambda) - 1 \right] \right\}. \tag{I8}$$

Note that in Eq. (I8) the λ sum includes the point $\lambda = 0$. To carry out the integration of the terms involving δ functions is of course trivial. For the remaining integration one proceeds as follows:

$$\int d^3h \exp\{-2\pi i \mathbf{h} \cdot \boldsymbol{\alpha}\} \frac{\exp(-\pi | \mathbf{h} |^2)}{\pi | \mathbf{h} |^2} = 2 \int_0^\infty dh \exp(-\pi h^2) \int_{-1}^1 d\chi \exp(-2\pi i h \alpha \chi)$$

$$= \frac{2}{\pi\alpha} \int_0^\infty \frac{dh}{h} \exp(-\pi h^2) \sin(2\pi h \alpha) = \frac{1}{\alpha} \operatorname{Erf}(\pi^{\frac{1}{2}} \alpha) = \frac{1}{\pi^{\frac{1}{2}} \alpha} \gamma(\tfrac{1}{2}, \pi\alpha^2),$$

where $\alpha \equiv | \boldsymbol{\alpha} |$.

We have therefore obtained

$$I_1(\mathbf{R})=\frac{ze}{\epsilon s}\frac{s^3}{(\beta+\gamma)r_1^2\sqrt{3}}\sum_{\lambda}\frac{\exp\{-\pi\mid\mathbf{h}_\lambda\mid^2\}}{\pi\mid\mathbf{h}_\lambda\mid^2}[\exp\{-2\pi i\mathbf{h}_\lambda\cdot\boldsymbol{\zeta}\}-\exp(-2\pi i\mathbf{h}_\lambda\cdot\{[\beta/(\beta+\gamma)]\mathbf{f}_3+\boldsymbol{\zeta}\})]$$
$$-\frac{ze}{\epsilon s(\pi^{\frac{1}{2}})}\left[\frac{1}{\mid\boldsymbol{\zeta}\mid}\gamma(\tfrac{1}{2},\pi\mid\boldsymbol{\zeta}\mid^2)-\frac{\gamma(\frac{1}{2},\pi\mid\boldsymbol{\zeta}+[\beta/(\beta+\gamma)]\mathbf{f}_3\mid^2)}{\mid\boldsymbol{\zeta}+[\beta/(\beta+\gamma)]\mathbf{f}_3\mid}\right]. \quad \text{(I9)}$$

If one carries out a limiting process which is not detailed here but wherein the charges are "modulated" in the $(\mathbf{a}_1, \mathbf{a}_2)$ plane by sinusoids of indefinitely large wavelength, one finds that the indeterminate term from the point $\lambda=0$ should be zero. Thus in Eq. (I9), the term $\lambda=0$ in the summation should be excluded.

Now we shall obtain an explicit expression for $\phi_a(\mathbf{R})$ which makes use of the sixfold symmetry of the lattice. First we need the following relations:

$$\mid\xi_k-\boldsymbol{\zeta}\mid=((r_1/s)^2(k_1^2+k_2^2-k_1k_2)+\{[2k_3(\beta+\gamma)-R]/s\}^2)^{\frac{1}{2}}, \quad \text{(I10)}$$

where

$$R\equiv\mathbf{R}\cdot\mathbf{a}_3/\mid\mathbf{a}_3\mid=\pm\mid\mathbf{R}\mid;$$

$$\left|\xi_k-\frac{\beta}{\beta+\gamma}\mathbf{f}_3-\boldsymbol{\zeta}\right|=\left\{\left(\frac{r_1}{s}\right)^2(k_1^2+k_2^2-k_1k_2)+\left[\frac{2k_3(\beta+\gamma)-2\beta-R}{s}\right]^2\right\}^{\frac{1}{2}}; \quad \text{(I11)}$$

$$\mid\boldsymbol{\zeta}\mid=\mid\mathbf{R}\mid/s; \quad \text{(I12)}$$

$$\mid\boldsymbol{\zeta}+[\beta/(\beta+\gamma)]\mathbf{f}_3\mid=s^{-1}\mid R+2\beta\mid; \quad \text{(I13)}$$

$$\mid\mathbf{h}_\lambda\mid^2=\lambda_3^2[s/(2\beta+2\gamma)]^2+(4s^2/3r_1^2)(\lambda_1^2+\lambda_2^2+\lambda_1\lambda_2); \quad \text{(I14)}$$

$$\mathbf{h}_\lambda\cdot\boldsymbol{\zeta}=\lambda_3\frac{R}{s}\frac{s}{2\beta+2\gamma}=\frac{\lambda_3R}{2\beta+2\gamma}; \quad \text{(I15)}$$

$$\mathbf{h}_\lambda\cdot\left(\boldsymbol{\zeta}+\frac{\beta}{\beta+\gamma}\mathbf{f}_3\right)=\frac{\lambda_3}{\beta+\gamma}(\beta+\tfrac{1}{2}R). \quad \text{(I16)}$$

It is in the above equations that we for the first time introduce the assumption that $\mathbf{R}\parallel\mathbf{a}_3$. This means of course that we are evaluating the potential along the line normal to the IHP which passes through the vacancy site. If one's interest were in finding the potential elsewhere, the above equations and the following development could be readily generalized. Insertion of Eq. (I10)–(I16) into (I9) and referring to (I2) leads to the following:

$$\phi_a(R)=-\frac{ze}{\epsilon(2\beta+R)}+\frac{ze}{\epsilon s}\sum_k{}'\left\{\frac{\operatorname{Erfc}\left(\pi^{\frac{1}{2}}\left\{(r_1/s)^2(k_1^2+k_2^2-k_1k_2)+\left[\frac{2k_3(\beta+\gamma)-R}{s}\right]^2\right\}^{\frac{1}{2}}\right)}{\left\{(r_1/s)^2(k_1^2+k_2^2-k_1k_2)+\left[\frac{2k_3(\beta+\gamma)-R}{s}\right]^2\right\}^{\frac{1}{2}}}\right.$$
$$\left.-\frac{\operatorname{Erfc}\left(\pi^{\frac{1}{2}}\left\{(r_1/s)^2(k_1^2+k_2^2-k_1k_2)+\left[\frac{2k_3(\beta+\gamma)-2\beta-R}{s}\right]^2\right\}^{\frac{1}{2}}\right)}{\left\{(r_1/s)^2(k_1^2+k_2^2-k_1k_2)+\left[\frac{2k_3(\beta+\gamma)-2\beta-R}{s}\right]^2\right\}^{\frac{1}{2}}}\right\}$$
$$+\frac{ze}{\epsilon s}\frac{s^3}{(\beta+\gamma)r_1^2\sqrt{3}}\sum_\lambda{}'\left\{\frac{\exp(-\pi\{[s/(2\beta+2\gamma)]^2\lambda_3^2+(4s^2/3r_1^2)(\lambda_1^2+\lambda_2^2-\lambda_1\lambda_2)\})}{\pi\{[s/(2\beta+2\gamma)]^2\lambda_3^2+(4s^2/3r_1^2)(\lambda_1^2+\lambda_2^2-\lambda_1\lambda_2)\}}\right.$$
$$\left.\times\left[\cos\left(\frac{\pi\lambda_3R}{\beta+\gamma}\right)-\cos\left(\frac{2\pi\lambda_3}{\beta+\gamma}(\beta+\tfrac{1}{2}R)\right)\right]\right\}-\frac{ze}{\epsilon s(\pi^{\frac{1}{2}})}\left\{\frac{\gamma[\frac{1}{2},\pi(R/s)^2]}{R/s}-\frac{\gamma\{\frac{1}{2},\pi[(R+2\beta)/s]^2\}}{(R+2\beta)/s}\right\}. \quad \text{(I17)}$$

We note here that as $R\to 0$, the term $-(ze/\epsilon s\pi^{\frac{1}{2}})\{\gamma[\frac{1}{2},\pi(R/s)^2]/(R/s)\}$ approaches $-2ze/\epsilon s$. This will be needed when we calculate the micropotential. Making use of the sixfold symmetry of the lattice we write

$$\phi_a(R)=-\frac{ze}{\epsilon(2\beta+R)}-\frac{ze}{\epsilon(\pi^{\frac{1}{2}})}\left\{\frac{\gamma[\frac{1}{2},\pi(R/s)^2]}{R}-\frac{\gamma[\frac{1}{2},\pi(R+2\beta)^2/s^2]}{R+2\beta}\right\}$$

$$+\frac{6ze}{\epsilon s}\sum_{k_3=-\infty}^{\infty}\sum_{k_2=1}^{\infty}\sum_{k_1=0}^{k_2-1}\left\{\frac{\operatorname{Erfc}\left(\pi^{\frac{1}{2}}\left\{(r_1/s)^2(k_1^2+k_2^2-k_1k_2)+\left[\frac{2k_3(\beta+\gamma)-R}{s}\right]^2\right\}^{\frac{1}{2}}\right)}{\left\{(r_1/s)^2(k_1^2+k_2^2-k_1k_2)+\left[\frac{2k_3(\beta+\gamma)-R}{s}\right]^2\right\}^{\frac{1}{2}}}\right.$$

$$\left.-\frac{\operatorname{Erfc}\left[\pi^{\frac{1}{2}}\left((r_1/s)^2(k_1^2+k_2^2-k_1k_2)+\left[\frac{2k_3(\beta+\gamma)-2\beta-R}{s}\right]^2\right)^{\frac{1}{2}}\right]}{\left\{(r_1/s)^2(k_1^2+k_2^2-k_1k_2)+\left[\frac{2k_3(\beta+\gamma)-2\beta-R}{s}\right]^2\right\}^{\frac{1}{2}}}\right\}$$

$$+\frac{ze}{\epsilon s}\sum_{\substack{k_3=-\infty\\ k_3\neq 0}}^{\infty}{}'\left\{\frac{\operatorname{Erfc}\left\{\pi^{\frac{1}{2}}\left|\frac{2k_3(\beta+\gamma)-R}{s}\right|\right\}}{\left|\frac{2k_3(\beta+\gamma)-R}{s}\right|}-\frac{\operatorname{Erfc}\left\{\pi^{\frac{1}{2}}\left|\frac{2k_3(\beta+\gamma)-2\beta-R}{s}\right|\right\}}{\left|\frac{2k_3(\beta+\gamma)-2\beta-R}{s}\right|}\right\}$$

$$+\frac{6ze}{\epsilon s}\frac{s^3}{(\beta+\gamma)r_1^2\sqrt{3}}\sum_{\lambda_3=-\infty}^{\infty}\sum_{\lambda_2=1}^{\infty}\sum_{\lambda_1=0}^{\lambda_2-1}\left\{\left[\cos\left(\frac{\pi\lambda_3R}{\beta+\gamma}\right)-\cos\left(\frac{2\pi\lambda_3}{\beta+\gamma}\beta+\tfrac{1}{2}R\right)\right]\right.$$

$$\left.\times\frac{\exp\left\{-\pi\left[\left(\frac{s}{2\beta+2\gamma}\right)^2\lambda_3^2+\frac{4s^2}{3r_1^2}(\lambda_1^2+\lambda_2^2-\lambda_1\lambda_2)\right]\right\}}{\pi\left[\left(\frac{s}{2\beta+2\gamma}\right)^2\lambda_3^2+\frac{4s^2}{3r_1^2}(\lambda_1^2+\lambda_2^2-\lambda_1\lambda_2)\right]}\right\}$$

$$+\frac{2ze}{\epsilon s}\frac{s^3}{(\beta+\gamma)r_1^2\sqrt{3}}\sum_{\lambda_3=1}^{\infty}\frac{\exp\left[-\pi\lambda_3^2\left(\frac{s}{2\beta+2\gamma}\right)^2\right]}{\pi\lambda_3^2\left(\frac{s}{2\beta+2\gamma}\right)^2}\left[\cos\left(\frac{\pi\lambda_3R}{\beta+\gamma}\right)-\cos\left(\frac{2\pi\lambda_3}{\beta+\gamma}\beta+\tfrac{1}{2}R\right)\right]. \quad \text{(I18)}$$

Specializing to the case $R=0(x=\gamma)$ yields the rapidly convergent result,

$$\phi_a(0)=-\frac{ze}{2\beta\epsilon}+\frac{6ze}{\epsilon s}\sum_{k_3=-\infty}^{\infty}\sum_{k_2=1}^{\infty}\sum_{k_1=0}^{k_2-1}\Bigg[\frac{\mathrm{Erfc}\{\pi^{\frac{1}{2}}[(r_1/s)^2(k_1^2+k_2^2-k_1k_2)+(4k_3^2/s_2)(\beta+\gamma)^2]^{\frac{1}{2}}\}}{[(r_1/s)^2(k_1^2+k_2^2-k_1k_2)+(4k_3^2/s^2)(\beta+\gamma)^2]^{\frac{1}{2}}}$$

$$-\frac{\mathrm{Erfc}(\pi^{\frac{1}{2}}\{(r_1/s)^2(k_1^2+k_2^2-k_1k_2)+(4/s^2)[(\beta+\gamma)k_3-\beta]^2\}^{\frac{1}{2}})}{\{(r_1/s)^2(k_1^2+k_2^2-k_1k_2)+(4/s^2)[(\beta+\gamma)k_3-\beta]^2\}^{\frac{1}{2}}}\Bigg]$$

$$+\frac{ze}{\epsilon s}\sum_{\substack{k_3=-\infty\\(k_3\neq 0)}}^{\infty}{}'\left\{\frac{\mathrm{Erfc}\{\pi^{\frac{1}{2}}\,|\,[2k_3(\beta+\gamma)]/s\,|\}}{|\,[2k_3(\beta+\gamma)]/s\,|}-\frac{\mathrm{Erfc}\{\pi^{\frac{1}{2}}\,|\,[2(\beta+\gamma)k_3-2\beta]/s\,|\}}{|\,[2(\beta+\gamma)k_3-2\beta]/s\,|}\right\}$$

$$+\frac{12ze}{\epsilon s}\frac{s^3}{(\beta+\gamma)r_1^2\sqrt{3}}\sum_{\lambda_3=1}^{\infty}\sum_{\lambda_2=1}^{\infty}\sum_{\lambda_1=0}^{\lambda_2-1}\Bigg[\left[1-\cos\left(2\pi\lambda_3\frac{\beta}{\beta+\gamma}\right)\right]$$

$$\times\frac{\exp(-\pi\{\lambda_3^2[s/(2\beta+2\gamma)]^2+(4s^2/3r_1^2)(\lambda_1^2+\lambda_2^2-\lambda_1\lambda_2)\})}{\pi\{\lambda_3^2[s/(2\beta+2\gamma)]^2+(4s^2/3r_1^2)(\lambda_1^2+\lambda_2^2-\lambda_1\lambda_2)\}}\Bigg]$$

$$+\frac{2ze}{\epsilon s}\frac{s^3}{(\beta+\gamma)r_1^2\sqrt{3}}\sum_{\lambda_3=1}^{\infty}\frac{\exp\{-\pi\lambda_3^2[s/(2\beta+2\gamma)]^2\}}{\pi\lambda_3^2[s/(2\beta+2\gamma)]^2}\left[1-\cos\left(2\pi\lambda_3\frac{\beta}{\beta+\gamma}\right)\right]-\frac{2ze}{\epsilon z}+\frac{ze}{2\beta\epsilon}\,\mathrm{Erf}\left(\pi^{\frac{1}{2}}\left|\frac{2\beta}{s}\right|\right). \quad \text{(I19)}$$

The final step needed in determining the micropotential is to subtract out the contribution of the line of self-images to the potential $\phi_a(R)$. This contribution, $S_0(R)$, is simply

$$S_0(R)=-\frac{ze}{\epsilon(2\beta+R)}+\frac{ze}{\epsilon}\sum_{k_3=1}^{\infty}\{[2k_3(\beta+\gamma)+R]^{-1}-[2k_3(\beta+\gamma)+2\beta+R]^{-1}$$

$$+[2k_3(\beta+\gamma)-R]^{-1}-[2k_3(\beta+\gamma)-2\beta-R]^{-1}\}. \quad \text{(I20)}$$

Next we make use of the identity

$$\sum_{n=1}^{\infty}[(n+x)^{-1}-(n+z)^{-1}]=\psi(z)-\psi(x)+z^{-1}-x^{-1},$$

where the tabulated[26] ψ function is further discussed by Erdelyi,[27] and is not to be confused with the potentials ψ_1, ψ_e, or ψ_a. We obtain

$$S_0(R)=-\frac{ze}{\epsilon(2\beta+R)}+\frac{ze}{\epsilon(2\beta+2\gamma)}\left[\psi\left(-\frac{2\beta+R}{2\beta+2\gamma}\right)-\psi\left(-\frac{R}{2\beta+2\gamma}\right)+\psi\left(\frac{2\beta+R}{2\beta+2\gamma}\right)-\psi\left(\frac{R}{2\beta+2\gamma}\right)\right].$$

But since $\psi(-z)=\psi(1-z)+z^{-1}$,

$$S_0(R)=-\frac{ze}{\epsilon(2\beta+R)}+\frac{ze}{2\epsilon(\beta+\gamma)}\left[\psi\left(\frac{2\beta+R}{2\beta+2\gamma}\right)-\psi\left(\frac{R}{2\beta+2\gamma}\right)\right.$$

$$\left.+\psi\left(1-\frac{R+2\beta}{2\beta+2\gamma}\right)-\psi\left(1-\frac{R}{2\beta+2\gamma}\right)+\frac{2\beta+2\gamma}{2\beta+R}-\frac{2\beta+2\gamma}{R}\right]. \quad \text{(I21)}$$

---

[26] H. T. Davis, *Tables of the Higher Mathematical Functions* (The Principia Press of Illinois, Inc., Evanston, Illinois, 1933), Vol. I.
[27] *Higher Transcendental Functions*, edited by A. Erdélyi (McGraw-Hill Book Company, Inc., New York, 1953), Vol. I.

As $R\to 0$, $S_0(R)$ goes over into

$$S_0(0)=-\frac{ze}{2\beta\epsilon}+\frac{ze\gamma_1}{\epsilon(\beta+\gamma)}+\frac{ze}{2\epsilon(\beta+\gamma)}\left[\psi\left(\frac{\beta}{\beta+\gamma}\right)+\psi\left(\frac{\gamma}{\beta+\gamma}\right)+\frac{\beta+\gamma}{\beta}\right]$$

$$=\frac{ze}{2\epsilon(\beta+\gamma)}\left[2\gamma_1+\psi\left(\frac{\beta}{\beta+\gamma}\right)+\psi\left(\frac{\gamma}{\beta+\gamma}\right)\right], \tag{I22}$$

where $\gamma_1\equiv$ Euler–Mascheroni constant $=0.57721566$. As special cases when $\beta=\gamma$, from $\psi(1/2)=-\gamma_1-2\ln 2$ we find $S_0(0)=-(ze\ln 2)/\beta\epsilon$; when $\gamma=2\beta$, $S_0(0)=-(ze\ln 3)/\epsilon\gamma$.

APPENDIX II: DETERMINATION OF $\mathfrak{F}_3\{\sum_{\boldsymbol{\lambda}}{}'\delta(\xi-\xi_{\boldsymbol{\lambda}})\exp(-2\pi i\boldsymbol{\kappa}\cdot\xi)\}$

Lemma 1:

$$\sum_{N=-\infty}^{\infty}\exp\{2\pi iNk\}=\sum_{\nu=-\infty}^{\infty}\delta(k-\nu).$$

Theorem 1:

$$\sum_{N=-\infty}^{\infty}f(x-N)=\sum_{\nu=-\infty}^{\infty}\exp(2\pi i\nu x)\int_{-\infty}^{\infty}f(\xi)\exp(-2\pi i\nu\xi)d\xi.$$

Proof:

$$f(x)=\int_{-\infty}^{\infty}dk\exp(2\pi ikx)\int_{-\infty}^{\infty}f(\xi)\exp(-2\pi ik\xi)d\xi.$$

$$\therefore f(x-N)=\int_{-\infty}^{\infty}dk\exp(-2\pi iNk)\exp(2\pi ikx)\int_{-\infty}^{\infty}f(\xi)\exp(-2\pi ik\xi)d\xi.$$

$$\sum_{N=-\infty}^{\infty}f(x-N)=\sum_{N=-\infty}^{\infty}\int_{-\infty}^{\infty}dk\exp(2\pi ikx)\exp(-2\pi iNk)\int_{-\infty}^{\infty}f(\xi)\exp(-2\pi ik\xi)d\xi.$$

By Lemma 1,

$$\sum_{N=-\infty}^{\infty}f(x-N)=\sum_{\nu=-\infty}^{\infty}\int_{-\infty}^{\infty}dk\exp(2\pi ikx)\delta(k-\nu)\int_{-\infty}^{\infty}f(\xi)\exp(-2\pi ik\xi)d\xi$$

$$=\sum_{\nu=-\infty}^{\infty}\exp(2\pi i\nu x)\int_{-\infty}^{\infty}f(\xi)\exp(-2\pi i\nu\xi)d\xi.$$

Lemma 2:

$$\sum_{\nu=-\infty}^{\infty}\delta(x-\nu)=\sum_{N=-\infty}^{\infty}\exp(2\pi iNx).$$

The proof follows from Theorem 1 by taking $f(x)\equiv\delta(x)$. Next we require the equations $\lambda_i=\mathbf{f}_i\cdot\mathbf{h}_{\boldsymbol{\lambda}}(i=1,2,3)$ where the vectors $\mathbf{f}$, $\mathbf{h}_{\boldsymbol{\lambda}}$, $\boldsymbol{\lambda}$ are defined in the text. Now one may proceed to Lemmas 3 and 4.

Lemma 3:

$$\sum_{\boldsymbol{\lambda}}\exp(2\pi i\mathbf{h}\cdot\xi_{\boldsymbol{\lambda}})=\sum_{\boldsymbol{\lambda}}\Big[\prod_{s=1}^{3}\delta(\mathbf{h}\cdot\mathbf{f}_s-\lambda_s)\Big].$$

Proof:

$$\sum_{\boldsymbol{\lambda}} \exp(2\pi i \mathbf{h}\cdot\boldsymbol{\xi}_{\boldsymbol{\lambda}}) = \sum_{\boldsymbol{\lambda}} \exp\Big[2\pi i \sum_{s=1}^{3} \lambda_s (\mathbf{h}\cdot\mathbf{f}_s)\Big]$$

$$= \sum_{\boldsymbol{\lambda}} \Big\{ \prod_{s=1}^{3} \exp[2\pi i \lambda_s (\mathbf{h}\cdot\mathbf{f}_s)] \Big\}$$

$$= \sum_{\lambda_1=-\infty}^{\infty} \sum_{\lambda_2=-\infty}^{\infty} \sum_{\lambda_3=-\infty}^{\infty} \exp[2\pi i \lambda_1 (\mathbf{h}\cdot\mathbf{f}_1)] \exp[2\pi i \lambda_2 (\mathbf{h}\cdot\mathbf{f}_2)] \exp[2\pi i \lambda_3 (\mathbf{h}\cdot\mathbf{f}_3)]$$

$$= \prod_{s=1}^{3} \Big\{ \sum_{\lambda_s=-\infty}^{\infty} \exp[2\pi i \lambda_s (\mathbf{h}\cdot\mathbf{f}_s)] \Big\}.$$

By Lemma 2 this becomes

$$\sum_{\boldsymbol{\lambda}} \exp(2\pi i \mathbf{h}\cdot\boldsymbol{\xi}_{\boldsymbol{\lambda}}) = \prod_{s=1}^{3} \sum_{\nu=-\infty}^{\infty} \delta(\mathbf{h}\cdot\mathbf{f}_s - \nu)$$

$$= \sum_{\nu_1=-\infty}^{\infty} \sum_{\nu_2=-\infty}^{\infty} \sum_{\nu_3=-\infty}^{\infty} \prod_{s=1}^{3} \delta(\mathbf{h}\cdot\mathbf{f}_s - \nu_s)$$

$$= \sum_{\boldsymbol{\nu}} \prod_{s=1}^{3} \delta(\mathbf{h}\cdot\mathbf{f}_s - \nu_s).$$

Lemma 4:

$$\sum_{\boldsymbol{\lambda}} \exp(2\pi i \mathbf{h}\cdot\boldsymbol{\xi}_{\boldsymbol{\lambda}}) = (1/v_f) \sum_{\boldsymbol{\lambda}} \delta(\mathbf{h} - \mathbf{h}_{\boldsymbol{\lambda}}).$$

Proof: From Lemma 3 one has

$$\sum_{\boldsymbol{\lambda}} \exp(2\pi i \mathbf{h}\cdot\boldsymbol{\xi}_{\boldsymbol{\lambda}}) = \sum_{\boldsymbol{\lambda}} \prod_{s=1}^{3} \delta\{(\mathbf{h} - \mathbf{h}_{\boldsymbol{\lambda}})\cdot\mathbf{f}_s\}.$$

Define the matrix A by the equations

$$\mathsf{A}_{ij} \equiv f_{ij},$$

where $f_{ij} \equiv j$th Cartesian component of $\mathbf{f}_i$.
Then

$$\mathbf{h}\cdot\mathbf{f}_i = (\mathsf{A}\mathbf{h})_i.$$

Noting that $\delta(\boldsymbol{\xi}) = \delta(\xi_x)\delta(\xi_y)\delta(\xi_z)$,

$$\prod_{s=1}^{3} \delta[(\mathbf{h} - \mathbf{h}_{\boldsymbol{\lambda}})\cdot\mathbf{f}_s] = \delta[\mathsf{A}(\mathbf{h} - \mathbf{h}_{\boldsymbol{\lambda}})].$$

But

$$\delta(\mathsf{A}\mathbf{x}) = \{\det\mathsf{A}\}^{-1}\delta(\mathbf{x}).$$

Since

$$\det\mathsf{A} - \mathbf{f}_1\cdot\mathbf{f}_2\times\mathbf{f}_3 = v_f,$$

$$\sum_{\boldsymbol{\lambda}} \exp(2\pi i \mathbf{h}\cdot\boldsymbol{\xi}_{\boldsymbol{\lambda}}) = (1/v_f) \sum_{\boldsymbol{\lambda}} \delta(\mathbf{h} - \mathbf{h}_{\boldsymbol{\lambda}}).$$

Lemma 5:

$$\mathfrak{F}_3\Big[\sum_{\boldsymbol{\lambda}} \delta(\boldsymbol{\xi} - \boldsymbol{\xi}_{\boldsymbol{\lambda}})\Big] = \sum_{\boldsymbol{\lambda}} \exp(2\pi i \mathbf{h}\cdot\boldsymbol{\xi}_{\boldsymbol{\lambda}})$$

Proof: From the definition of the Fourier transform,

$$\mathfrak{F}_3[\sum_{\lambda}\delta(\xi-\xi_\lambda)]=\sum_{\lambda}\mathfrak{F}_3[\delta(\xi-\xi_\lambda)]$$

$$=\sum_{\lambda}\exp(-2\pi i\mathbf{h}\cdot\xi_\lambda)=\sum_{\lambda}\exp(2\pi i\mathbf{h}\cdot\xi_\lambda).$$

Theorem 2:

$$\mathfrak{F}_3[\sum_{\lambda}\delta(\xi-\xi_\lambda)]=(1/v_f)\sum_{\lambda}\delta(\mathbf{h}-\mathbf{h}_\lambda).$$

The proof follows immediately from Lemmas 4 and 5.

Lemma 6:

$$\mathfrak{F}_3[f(\xi)\exp(2\pi i\mathbf{k}\cdot\xi)]=G(\mathbf{h}-\mathbf{k}),$$

where

$$\mathfrak{F}_3[f(\xi)]=G(\mathbf{h}).$$

Theorem 3 follows.

Theorem 3:

$$\mathfrak{F}_3\{\sum_{\lambda}\delta(\xi-\xi_\lambda)\exp(-2\pi i\mathbf{k}\cdot\xi)\}=(1/v_f)\sum_{\lambda}\delta(\mathbf{h}+\mathbf{k}-\mathbf{h}_\lambda).$$

Corollary:

$$\mathfrak{F}_3[\sum_{\lambda}{}'\delta(\xi-\xi_\lambda)\exp(-2\pi i\mathbf{k}\cdot\xi)]=(1/v_f)\sum_{\lambda}\delta(\mathbf{h}+\mathbf{k}-\mathbf{h}_\lambda)-1,$$

which was to be determined.